

In-field Torsion Measurements on Solar Trackers Using Fiber Optic Sensors

D. Leandro¹, M. Bravo¹, A. Judez¹, J. Mariñelarena¹, F. Falcone¹, A. Loayssa¹, M. Lopez-Amo¹
S. Jimenez², A. Achaerandio²

¹Dpt. of Electrical Electronic and Communication Engineering and Institute of Smart Cities (ISC), Public University of Navarra, 31006 Pamplona, Spain

²STI Norland S.L., Avda. Sancho el Fuerte, 26. Oficinas 1, 31008, Pamplona, Spain

*Corresponding author: daniel.leandro@unavarra.es

Abstract: In-field torsion measurements on solar trackers using fiber Bragg gratings are presented. 45 FBG sensors have been deployed in an operational solar energy plant to study the mechanical response of the structure to wind.

OCIS codes: (060.2370) Fiber optics sensors; (060.3735) Fiber Bragg gratings, (350.6050) Solar energy

1. Introduction

Nowadays, there is an increasing concern among the international community about climate change and its unwanted side-effects. Despite any other considerations, there is a general agreement that renewable energies should be further developed to limit the consumption of fossil fuels, which would consequently mitigate global warming and reduce pollution. In this context, solar energy (particularly photovoltaic) is one of the most important alternatives, and it is the one with the fastest growth, as it is evidenced by a 100% increase in the capacity installed in 2019 in EU with respect to 2018. Moreover, recent reports predict that it has been more new solar capacity installed in EU than any other power generation technology in 2019 [1]. Photovoltaic (PV) power stations mostly rely on the use of PV panels combined with sun-trackers. These trackers are designed to follow the sun's trajectory to keep the PV panel operating at an optimal position. There are numerous types of trackers and configurations deployed in PV power stations, but all of them strive for an increase in efficiency and operating time to maximize the power generation. Consequently, a lot of effort has been put on improving the efficiency and the long-term reliability of the trackers [2].

The effects of weather on trackers, particularly the failures caused by wind, were the most frequent cause of insurance claims in PV power plants between 2011-2015 [3]. Conventionally, the analysis of the effects of wind in the design of solar trackers mainly consider the static-load information obviating dynamic amplification effects. However, it has been noted that dynamic wind loads during aeroelastic instability events can be five times higher than static wind loads [4]. Therefore, the acquisition of appropriate information of the state of the trackers as a function of wind speed and direction is of key importance to avoid damage in the installations. Moreover, actual safety protocols sometimes over-react to the effects of wind. Thus, an adequate evaluation of the trackers condition could extend the operating time, increasing the production as a consequence. To achieve this, fiber optic sensors stand out over conventional approaches due to their unique properties such as being electromagnetically passive, their small size and light weight among others [5]. It is of special interest in this application the ability to remotely interrogate the sensors due to low attenuation of the fiber, so no power supply is required at the location of the sensors.

In this context, this study is framed inside a project devoted to analyze the effects of wind in solar trackers in-field. The project devises the installation of point fiber optic sensors to monitor the torsion suffered by the structure. The torsion sensors have been located at critical positions which after an analysis, could act as indicators of the state of the whole structure. Specifically, this work presents the initial results of torsion measured in solar trackers using fiber Bragg gratings (FBGs). Also, it describes the setup of the network used, and the configuration of the torsion sensors. These preliminary results allowed the validation of the sensors to continue the analysis of wind-related events.

2. Aim and principle of operation

As aforementioned, this work is framed within a research project aimed to study the effects of wind on photovoltaic (PV) trackers. In this regard, fiber optic sensors are used to monitor the mechanical behavior of the different sections of the trackers. In particular, it is of key importance the relationship between wind and bending or torsional moment in the structure. The development based on the classic theories of Euler-Bernoulli and Saint Venant's to calculate the torsion of a beam using can be straightforwardly adapted to FBGs by locating them at a $\pm 45^\circ$ angle [6].

The PV trackers structure consists of a set of beams with a central torque tube beam that supports the array of solar panels. Thus, assuming two strain point sensors placed at a $\pm 45^\circ$ angle with respect to the longitudinal axis of the beam, the torsion moment M_T can be derived as

$$M_T = (\varepsilon_1 - \varepsilon_2) W_T G, \quad (1)$$

where ε_1 and ε_2 are strains obtained from sensor 1 and 2 respectively, W_T is the torsion resistant module and G is the transversal Shear modulus (which is given by the material). The values employed are $G = 85.000$ (N/mm²) and $W_T = 56.442$ or 73.700 mm³ depending on the thickness of the beam in which the sensors are attached. It is important to note that due to the nature of the detection principle, the temperature fluctuations are self-compensated so there is no need of compensation in the case of torsion monitoring. However, temperature sensors have been included in the network just to compensate regular strain/bending measurements.

3. Experimental setup

A picture of the PV power station located in Bardenas Reales (Spain) where the study has been performed can be seen in Fig. 1. The solar trackers under study include the first three rows, with an approximate length of 60 m. The sensor network is composed by a 4-channel fiber optic sensors interrogator Micronoptics SM130 and a 4-channel optical switch (connected to one channel of the interrogator) placed in a control room about 1.5 km away from the PV trackers. In this manner, up to 7 arrays can be measured, four corresponding to the switch channels plus the three remaining interrogator channels. Each array comprises 6-7 FBGs, which are wavelength-multiplexed in the C-band. Figure 2 shows the schematic of the sensor locations in the structure that consists of 19 torsion sensors (2 FBG each), 2 strain sensors and 5 temperature sensors for temperature monitoring and compensation of the strain sensors. Consequently, a total of 45 FBG sensors are employed in the study.

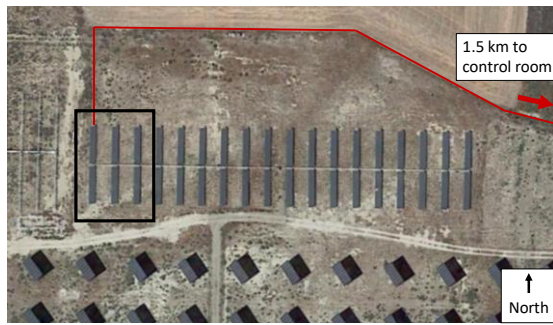


Fig. 1. Photograph of the monitored PV trackers. The square shows the 3 linear trackers under study. The red line represents the path of the fiber optic to the control room. Map provided by Google – Gobierno de Navarra and Inst. Geográfico Nacional.

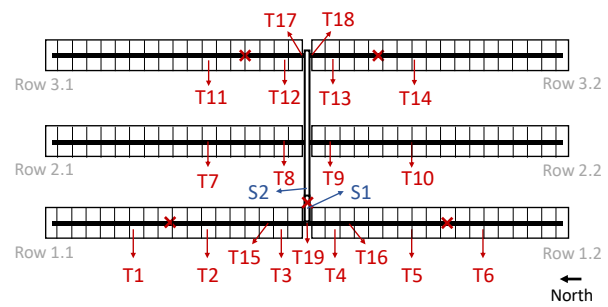


Fig. 2. Schematic setup of the sensor network. Red T+number represents couples of FBGs torsion sensors; blue S+number are strain sensors and red crosses represents temperature sensors.

The location of each sensor has been selected to obtain specific information from critical points of the structure. In a simplified manner, the PV trackers can be seen as a motor linked to a connecting rod which in turn is linked to the beams supporting the PV panels. In this manner, the most representative positions have been defined as the joints between the six beams that form the first row, and the four joints closer to the connecting rod in the second and third row. Also, it is monitored the torsion in the beams closer to the connecting rod at the first and third row. Additionally, the torsion and axial strain is measured in the joint between the connecting rod and the beam in the first row. Finally, it is assessed the strain in the connecting rod. A summary of the sensors installed can be seen in Table 1. Note that all the torsion sensors consist of two FBG placed with a relative angle of $\pm 45^\circ$ with respect to the longitudinal axis of the structure as depicted in Figure 3 (a).

Table 1. Summary of the installed sensors and the W_T parameter (torsion sensors).

| Code | Location | Measurand | W_T |
|-------------|---|-------------|-----------------------|
| T1 to T14 | Joint between supporting beams | Torsion | 56442 mm ³ |
| T15 T16 | Supporting beams | Torsion | 56442 mm ³ |
| T17 T18 | Supporting beams | Torsion | 73700 mm ³ |
| T19 | Connecting rod | Torsion | 73700 mm ³ |
| S1 | Joint between connecting rod and supporting beams | Strain | - |
| S2 | Connecting rod | Strain | - |
| Temp 1 to 5 | Next to S1-S2 and supp. Beams | Temperature | - |



Fig. 3. Picture of three installed sensors: a) T1 b) S1 c) S2

4. Results

Initially, a number of experiments were carried out to test the proper operation of the system and to analyze the impact of torsion in the structure. The detection of all the sensors was performed successfully after the installation. Then, the wavelength shift of each FBG is monitored and treated accordingly. I.e., in the case of torsion sensors, the strain measured in the corresponding pair of FBGs is converted to torsion using equation 1. In the case of regular strain sensors, the wavelength shift is compensated using a temperature sensor before converting it to axial strain.

The most illustrating experiments include the application of torsion to different locations of the structure. In these experiments, torsion was applied to several positions of the supporting beams by placing weight. For example, Fig. 4 shows the results retrieved at 100 Hz in which three torsion moments were incrementally applied to T6 and T5 consecutively. In the first case, as expected, the torsion measured in T6 is higher. It is also worth noticing that the torsional moment is transmitted to the elements in the direction to the central rod (from T6 to T5 and T4). This is probably because the closer to the central rod, the higher is the resistance to twist induced by the structure, since the central rod is acting as a fixed end. This effect is more evident when the torsion was applied to T5 (Fig. 4, starts in 30s). In this case T6 suffers almost no torsion because it is placed on a joint between two supporting beams, one of them being at the loose end of the structure. This is also in accordance with the results obtained from the other cases. Another set of experiments verified that the torsion is not transmitted through the connecting rod. Fig. 5 shows the results of row 3 when torsion is applied to T11 and T13 respectively. In the first case, torsion is applied to T11 and as expected, there is no signal change in T13 because the connecting rod does not transmit the force. Equivalently, when torsion is present at T13, T11 and T12 remain stable. It should be noted that there is a certain non-elastic behavior in the structure since torsion does not recover to the initial values after the release of the weight. This is evidenced by T5 in Fig. 5 after the second excitation. It was noted that further excitations can cause the release of the torsional moment. That could be due to the dry friction induced by the rotating joints that link the beams to the pillars of the structure; however, further work is required in this respect.

After the verification of the sensors, it was initiated a measurement campaign under real conditions. Fig. 6 depicts a sample of the torsion measured in row 1 from 26th to 30th September 2019. The weather during this period remained calm, with winds under 4 m/s, temperatures ranging from 15 to 30 °C and no rainfall. A moving average of 10 samples has been applied to the measurements for the sake of clarity. It can be seen the existence of daily patterns. These could be due to daily temperature variations, daily positioning of the trackers or daily wind patterns among others. All these aspects, with especial consideration to the relationship between wind speed/direction with torsion, are under investigation at the moment.

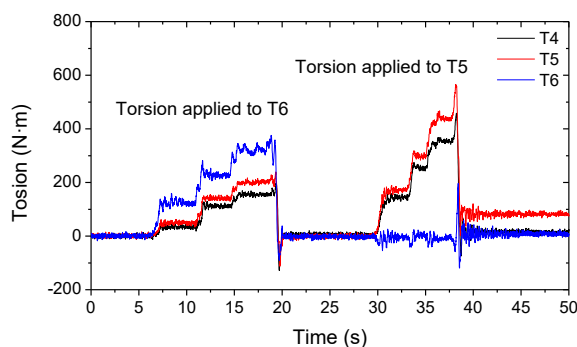


Fig. 4. Torsion measured in T4, T5 and T6 sensors when torsion is applied to T6 and to T5.

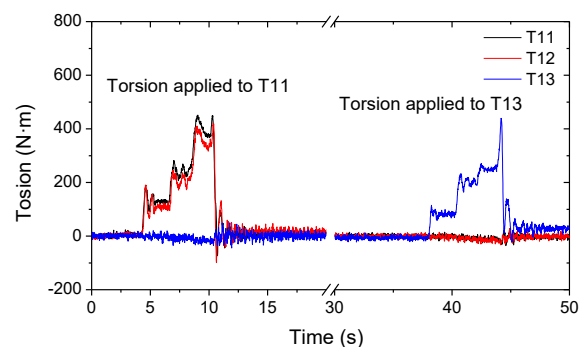


Fig. 5. Torsion measured in T11, T12 and T13 sensors when torsion is applied to T11 and to T13.

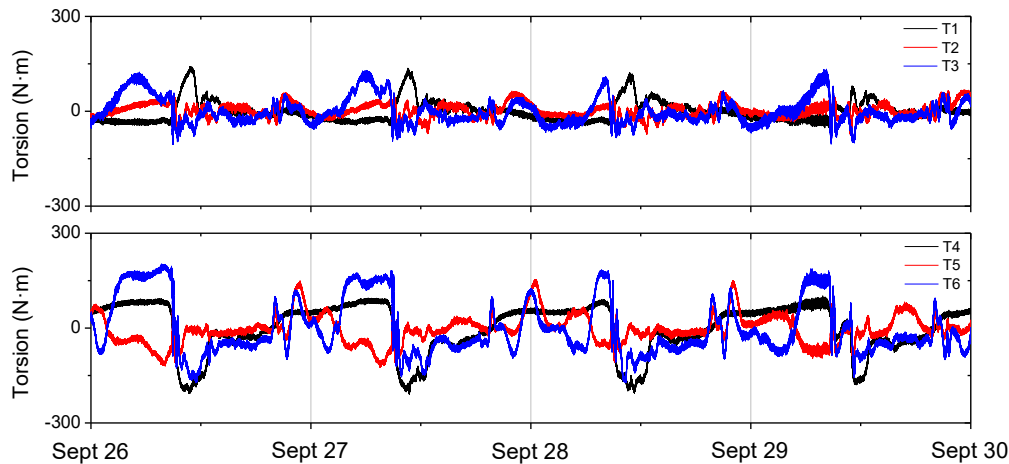


Fig. 6. Results retrieved during the period 26th-30th September 2019 for (upper) row 1.1 and (lower) row 1.2.

4. Conclusions

In this study, preliminary torsion measurements of solar trackers using FBGs have been presented. Each torsion sensor is comprised by two FBGs placed with a $\pm 45^\circ$ angle offset with respect to the axis of the beam. This configuration allows the detection of torsion without the influence of temperature. Moreover, extra FBGs have also been included in the network to estimate axial strain and temperature at certain positions. A total of 45 FBGs have been deployed to implement 19 torsion, 2 axial strain and 5 temperature sensors. These sensors have been mainly placed on critical points of three rows of solar trackers, such as joints between beams, but also on secondary ones such as on the beams themselves. On one side this allows to infer a general status of the whole structure. On the other side, this could detect the points of the structure that are affected the most by wind gusts.

A series of tests have been carried out to validate the performance of the sensors. In these experiments, torsion was applied at different positions of the structure. The detected wavelength shift at each sensor showed a correct behavior, validating the successful operation of the network. Finally, a sample of measurements recorded under real conditions have been presented. These initial results seem promising and further work is being done to correlate the torsion suffered by the structure with possible causes, especially the direction and speed of the wind. This information would be highly valuable to improve the safety and efficiency in PV solar plants.

Funding. This work was supported by the Gobierno de Navarra project WINDSOLAR (0011-1365-2017-000122), the Spanish AEI project TEC2016-76021-C2, FEDER Funds, ISC talent grant, and the European Union's Horizon 2020 research and innovation programme under the Marie Skłodowska-Curie grant agreement No 838143.

5. References

- [1] [EU-28 annual solar PV installed capacity 2000-2019], Solar Power Europe (Dec 2019).
- [2] W. Nsengiyumva, S. G. Chen, L. Hu, X. Chen, "Recent advancements and challenges in Solar Tracking Systems (STS): A review," *Renewable and Sustainable Energy Reviews*, 81(1), 250-279 (2018).
- [3] K. Pickerel, "How the solar industry is responding to the increasing intensity of natural disasters," *Solar Power World* (Jan 2018).
- [4] C. Rohr, P. A. Bourke, D. Banks, "Torsional instability of single-axis solar tracking systems," *Proc. of the 14th International Conference on Wind Engineering*, 21–26 (2015).
- [5] J.M. Lopez-Higuera, *Handbook of Optical Fibre. Sensing Technology*; John Wiley&Sons." Inc.: Hoboken, NJ, USA (2002).
- [6] Y. Wang, L. Liang, Y. Yuan, G.Xu, F. Liu, "A two fiber bragg gratings sensing system to monitor the torque of rotating shaft," *Sensors*, 16(1), 138 (2016).